A Numerical Experiment on the Zonal Jet Formation in 2-D Turbulent Flow on a Beta-Plane

Shigeo Yoden and Jitsuko Hasegawa

Department of Geophysics, Kyoto University

A series of numerical experiments on two-dimensional decaying turbulence are performed for a non-divergent barotropic fluid on a β-plane (a tangential plane to a rotating planet with the effect of latitudinally varying Coriolis parameter f) in order to survey the nature of zonal jet formation from random initial fields. A parameter $\beta \equiv df/d\phi$ (ϕ: latitude) is swept systematically to show the dependence of latitudinal structure of the zonal jet on its magnitude. Dynamics of such zonal jet formations is investigated with a weakly nonlinear Rossby wave-zonal flow interaction theory.

1 Introduction

An interesting feature of two-dimensional turbulence, in contrast to ordinary three-dimensional turbulence, is the emergence of isolated coherent vortices found by McWilliams [1, 2]. Formation of such coherent vortices is due to a self-organizing mechanism involved in the disorder two-dimensional motion. As an application to geophysical fluid, Rhines [3] firstly studied the two-dimensional turbulence on a β-plane, which is a tangential plane to a rotating planet with the effect of latitudinally varying Coriolis parameter [4], to understand the effect of differential rotation of the planet on the two-dimensional turbulence. His numerical result showed anisotropic growth of flow field and emergence of alternating bands of mean zonal flow. These features due to the β-effect have been reconfirmed in recent numerical studies with much higher resolution models [5, 6]. They noticed the zonal jet structures persist over many eddy turnover times. Extremely persistent zonal jets are also observed in quasigeostrophic two-layer β-plane turbulence forced by an imposed unstable vertical shear [7].

Williams [8] took account of the exact spherical geometry in his numerical experiment on forced two-dimensional turbulence, aiming at a reproduction of the zonal band structure of Jovian atmosphere due to the β-effect. He obtained a clear band structure of zonal flow for a stochastic vorticity forcing. However, both longitudinal periodicity and equatorial symmetry were assumed in his experiment to reduce the computational domain to 1/16 of the entire sphere. Advancement of computing facilities in 1990's enabled us to do these computations with higher resolutions in full spherical geometry [9-15]. In the decaying turbulence experiments [9, 14], the spontaneous formation of the zonal jets was found in mid- and low-latitudes

for strong rotation cases, in addition to the emergence of a westward circumpolar vortex in high-latitudes. Such formation of persistent zonal jets was also observed in the forced turbulence experiment [11, 13].

Pattern formation in two-dimensional turbulence on a rotating sphere may be applied for understanding some phenomena in the real geophysical fluids. The formation of zonal jets from a random flow field has been considered as a mechanism to explain the band structures in the atmospheres on the giant outer planets such as Jupiter, Saturn, Uranus and Neptune [8, 16]. Westward zonal flow in high latitudes in the sun [17] has superficial similarity to the circumpolar vortex obtained in our experiments [9, 11]. Recently numerical study on the solar tachocline was also done by investigating freely evolving stratified turbulence in a thin rotating spherical shell [18]. Annular variability observed in both hemispheres of the atmosphere [19, 20] is a modulation in the strength of the circumpolar vortex in the troposphere and lower stratosphere with intraseasonal and interannual time scales. Variations of the mean zonal jets with significant barotropic components have much connection with time variations of meridional and vertical potential vorticity (PV) flux [21], and key dynamics of the annular variability may be identical with that of the formation of the present circumpolar vortex [22].

Rhines [23] described fundamental mechanisms for the formation of zonal jets on rotating spheres in some circumstances. One example which is associated with the present subject is random external stirring of fluid which becomes organized by the β-effect into jets. The role of Rossby waves in angular momentum redistribution may be important after full nonlinear upward cascade of turbulent energy in small scales [24].

In this study, we perform a series of numerical experiments on two-dimensional decaying turbulence for a non-divergent barotropic fluid on a β-plane in order to survey the nature of zonal jet formation from random initial fields. We choose a β-plane geometry with doubly periodic boundary conditions, because of simpler dynamical situation than rotating sphere. Latitudinal dependence of the β-effect and spherical geometry introduce some difficulty to understand the dynamics, although these characteristics are more relevant to the atmospheres.

2 Numerical Model and Experiments

Freely-evolving two-dimensional non-divergent flow on a β-plane is governed by the following nondimensionalized vorticity equation:

$$\frac{\partial \zeta}{\partial t} + u\frac{\partial \zeta}{\partial x} + v\frac{\partial \zeta}{\partial y} + \beta v = -\nu_2 \Delta^2 \zeta, \tag{1}$$

where $\zeta(x, y, t)$ is the vertical component of vorticity ($\equiv \partial v/\partial x - \partial u/\partial y$), (u, v) horizontal velocity ($\equiv (dx/dt, dy/dt)$), (x, y) eastward and northward coordinates, t the time, Δ the horizontal Laplacian, β nondimensionalized beta ($f = f_0 + \beta y$), and ν_2 nondimensionalized hyperviscosity coefficient. As $\nu_2 \to 0$, this equation gives the conservation low of PV (in the present case it is equivalent to absolute vorticity) $q \equiv \zeta + f$ following Lagrangian motion. If we introduce a streamfunction $\psi(x, y, t)$ ($u = -\partial\psi/\partial y, v = \partial\psi/\partial x$), Eq.(1) can be written as

$$\frac{\partial}{\partial t}\Delta\psi + J(\psi, \Delta\psi) + \beta\frac{\partial \psi}{\partial x} = -\nu_2 \Delta^3 \psi, \tag{2}$$

where $J(A, B)$ is the horizontal Jacobian. As for the boundary condition, we assume a periodic boundary condition in both directions with 2π: $\psi(x, 0, t) = \psi(x, 2\pi, t)$ and $\psi(0, y, t) = \psi(2\pi, y, t)$.

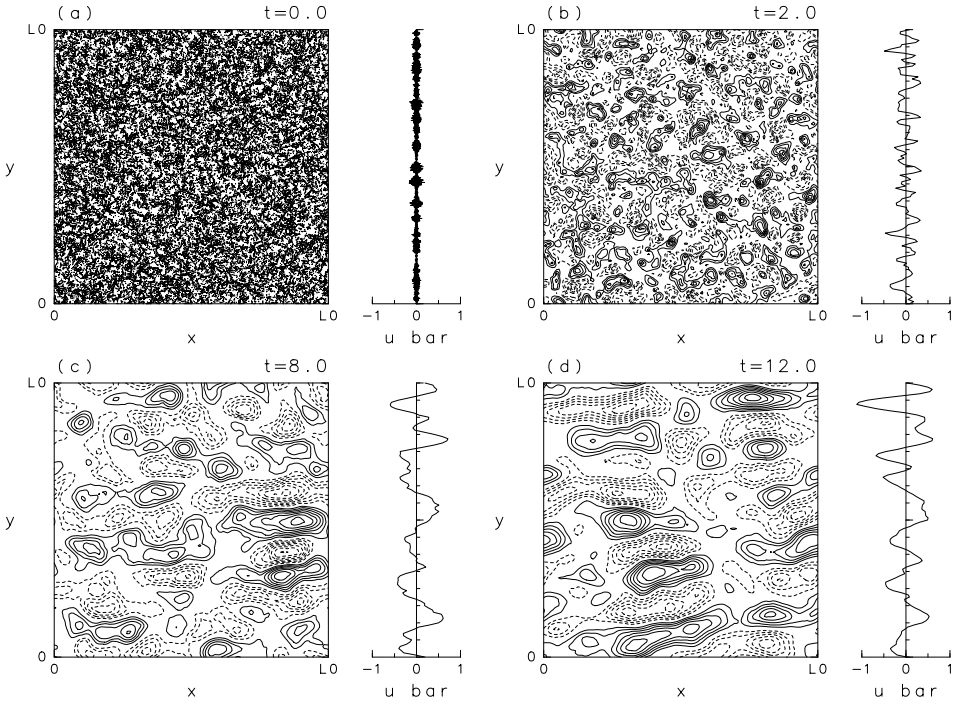

Figure 1: Time evolution of the streamfunction $\psi(x, y, t)$ and the zonal mean zonal flow $[u](y, t)$ for $t = 0$ (a), 2 (b), 8 (c), and 12 (d) in the run of $\beta = 100$. Negative contours of ψ are drawn with broken lines.

A spectral model of Eq.(2) is constructed by a double Fourier expansion ($\propto \exp[i(kx+ly)]$) of ψ with the truncation wavenumber $k_m = l_m = 1024$. A spectral transform method [25] is used to compute the nonlinear Jacobian term; grids for the transformation is 4096×4096. Time evolution of $\psi(x, y, t)$ is computed from an initial random flow field, of which one-dimensional kinetic energy spectrum for a scalar wavenumber κ is given by

$$E(\kappa, t=0) = \frac{A\kappa^{\gamma/2}}{(\kappa + \kappa_0)^{\gamma}}, \tag{3}$$

with $\gamma = 1000$ and $\kappa_0 = 226$. A constant A is set so that the total kinetic energy is $1/2$ at $t = 0$. Time integrations are done until $t = 12$ by the fourth-order Runge-Kutta method with the time increment of $\Delta t = 4 \times 10^{-4}$. Ten values of β are taken as an experimental parameter: $\beta = 2^{n-1} \times 100$ ($n = 1, 2, \cdots, 10$). Even for the smallest value of $\beta = 100$, a characteristic wavenumber $k_\beta = \sqrt{\beta/U}$ with $U \sim 1$, which gives a scale of transition from turbulence to Rossby-wave motion, is much larger than the lowest wavenumber 1. Large value of k_β supports the soundness of the periodic boundary condition. The hyperviscosity coefficient is set to $\nu_2 = 1 \times 10^{-10}$. All of the computations are done in double precision.

3 Results

Figure 1 shows time evolution of the streamfunction $\psi(x, y, t)$ and the zonal mean zonal flow $[u](y, t)$ for the run of $\beta = 100$. Here $[a] = \dfrac{1}{2\pi}\displaystyle\int_0^{2\pi} a\, dx$. Initially the flow field is isotropic, but

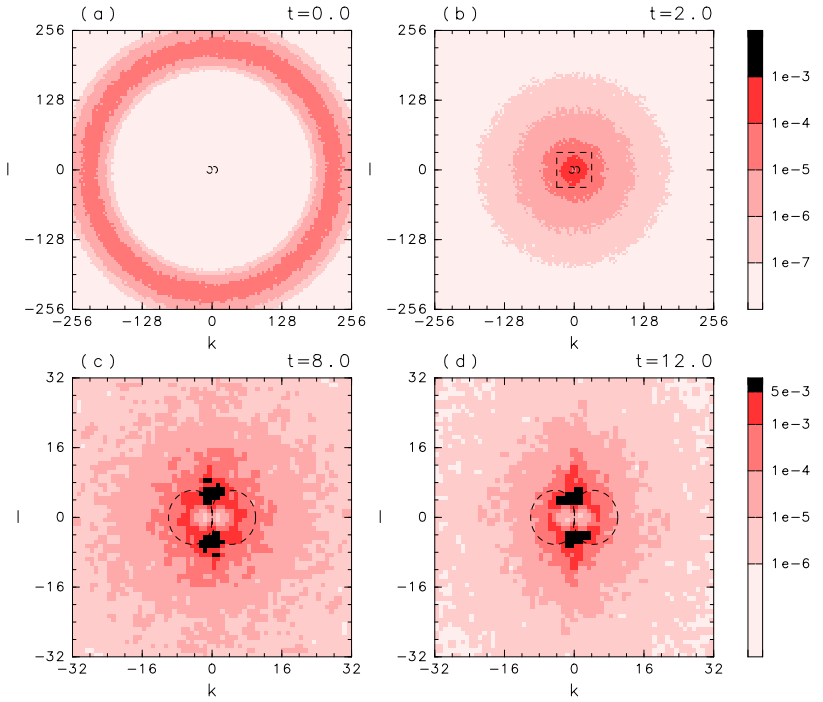

Figure 2: Time evolution of two-dimensional energy spectrum for $t = 0$ (a), 2 (b), 8 (c), and 12 (d). Note the wavenumber ranges and tone values are different between (a,b) and (c,d). Broken lines give the "dumbbell" of anisotropic wave-turbulence boundary in wave vector space. See text for details.

vortices become elongated in zonal direction. By $t = 8$, the zonal wavenumber 1 component dominates, and typical Rossby-wave motion can be seen in the animations of the streamfunction field. At the same time, the zonal mean zonal flow develops, and its latitudinal scale becomes large. The meridional profile of $[u]$ looks similar between $t = 8$ and 12, which is indicative of the persistence of the zonal mean zonal flow.

Time evolution of two-dimensional energy spectrum is shown in Fig.2 for the same run of $\beta = 100$. Upward energy cascade to lower wavenumbers takes place initially, and the spectrum is roughly dependent only on the scalar wavenumber $\kappa = \sqrt{k^2 + l^2}$ at $t = 2$, indicating isotropic flow field in small scales. However, it is not isotropic in large scales. The two-dimensional spectrum shows anisotropic distribution in low wavenumbers as pointed out by Vallis and Maltrud [6]. Broken lines in Fig.2 give the "dumbbell" of anisotropic wave-turbulence boundary in wave vector space introduced by them:

$$(k, l) = k_\beta(\cos^{3/2}\theta, \cos^{1/2}\theta \sin\theta), \qquad \theta = \tan^{-1}(l/k). \tag{4}$$

Note that the largest components of the spectrum are inside the boundary, although the low-energy region shows a dumbbell shape in it. These are consistent with the findings in the spherical geometry experiments [12, 13].

Parameter dependence on β is summarized as the time evolution of one-dimensional energy spectrum(Fig.3). The spectral peak exists at a lower wavenumber than k_β, and shifts to higher wavenumber as β increases. The one-dimensional spectrum shows a power low roughly between the peak and κ_0, and the slope steepens as β increases: $E(\kappa) \propto \kappa^\alpha$, $\alpha \sim -4$ for $\beta = 400$, while

$\alpha \sim -5$ for $\beta = 12800$ at $t = 12$. Energy density at the lowest wavenumbers is much smaller than the peak value, indicating the influence of the periodic boundary condition is weak in these experiments.

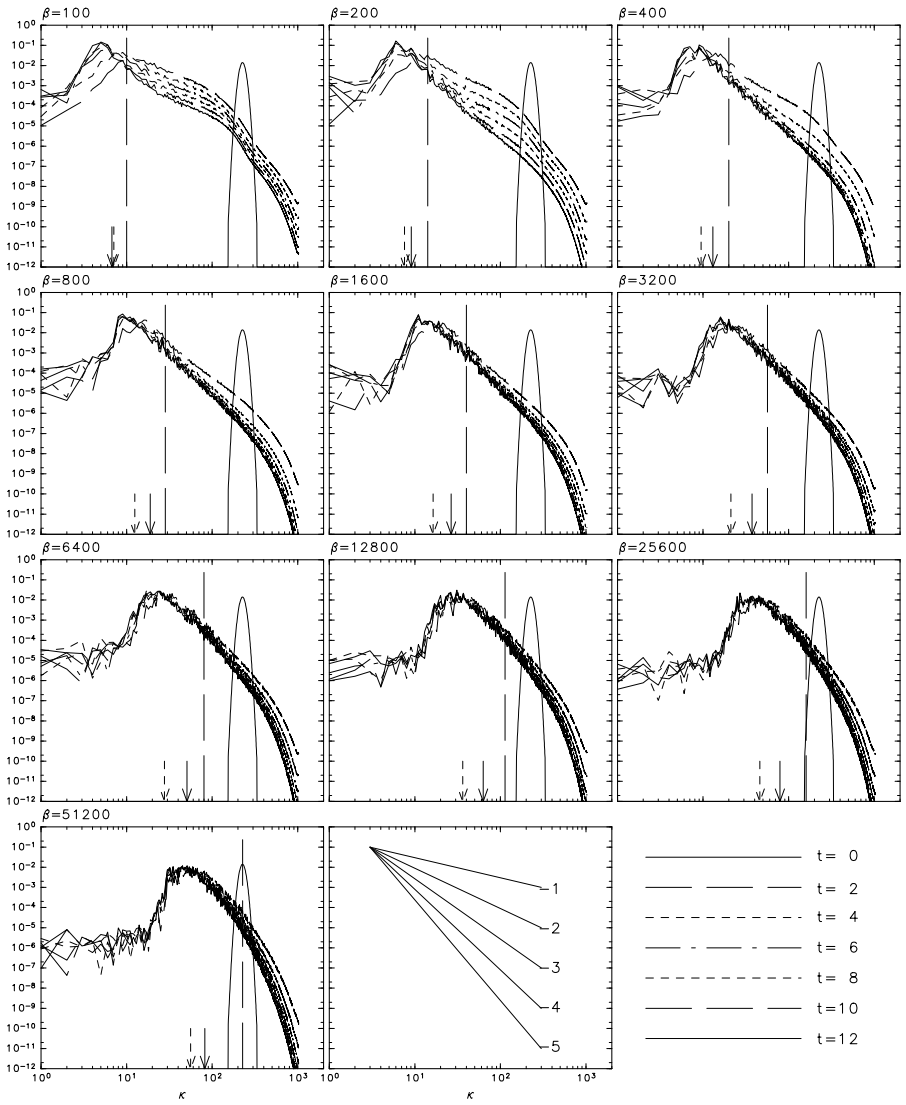

Figure 3: Time evolution of one-dimensional energy spectrum for 10 values of β. Vertical broken line gives k_β. Broken arrow on the abscissa gives the energy centroid wavenumber at $t = 12$, and solid one does that only for $k = 0$ component.

In order to relate the present results with the real geophysical fluid, we introduce a length scale of $L = 5 \times 10^6$ m, which is roughly the radius of the earth, and the velocity scale $U = 10$ ms^{-1}. Then a dimensional value of beta becomes $\beta^* = (U/L^2)\beta$, and $\beta^* = 4 \times 10^{-11}$ m^{-1}s^{-1} for $\beta = 100$. This value is comparable to that in mid-latitudes of the earth. If we take $8L$ as a length scale and pick up only 1/8 in both directions of x and y, then the subset can be regarded as another series of experiments with smaller value of beta $\beta^* = (U/L^2)\beta/64$ for the same domain size with dimension.

Figure 4 shows meridional profiles the zonal mean zonal flow $[u](y,t)$ for 16 values of β^*, with four values of overlapping ($\beta^* = 4 \times 10^{-11} \sim 3.2 \times 10^{-10}$ m^{-1}s^{-1}). Meridional scale of the mean zonal flow decreases as β^* decreases. The maximum value of $|[u]|$ is about 10 ms^{-1}, except for three cases of the largest β in which k_β is not very different from κ_0.

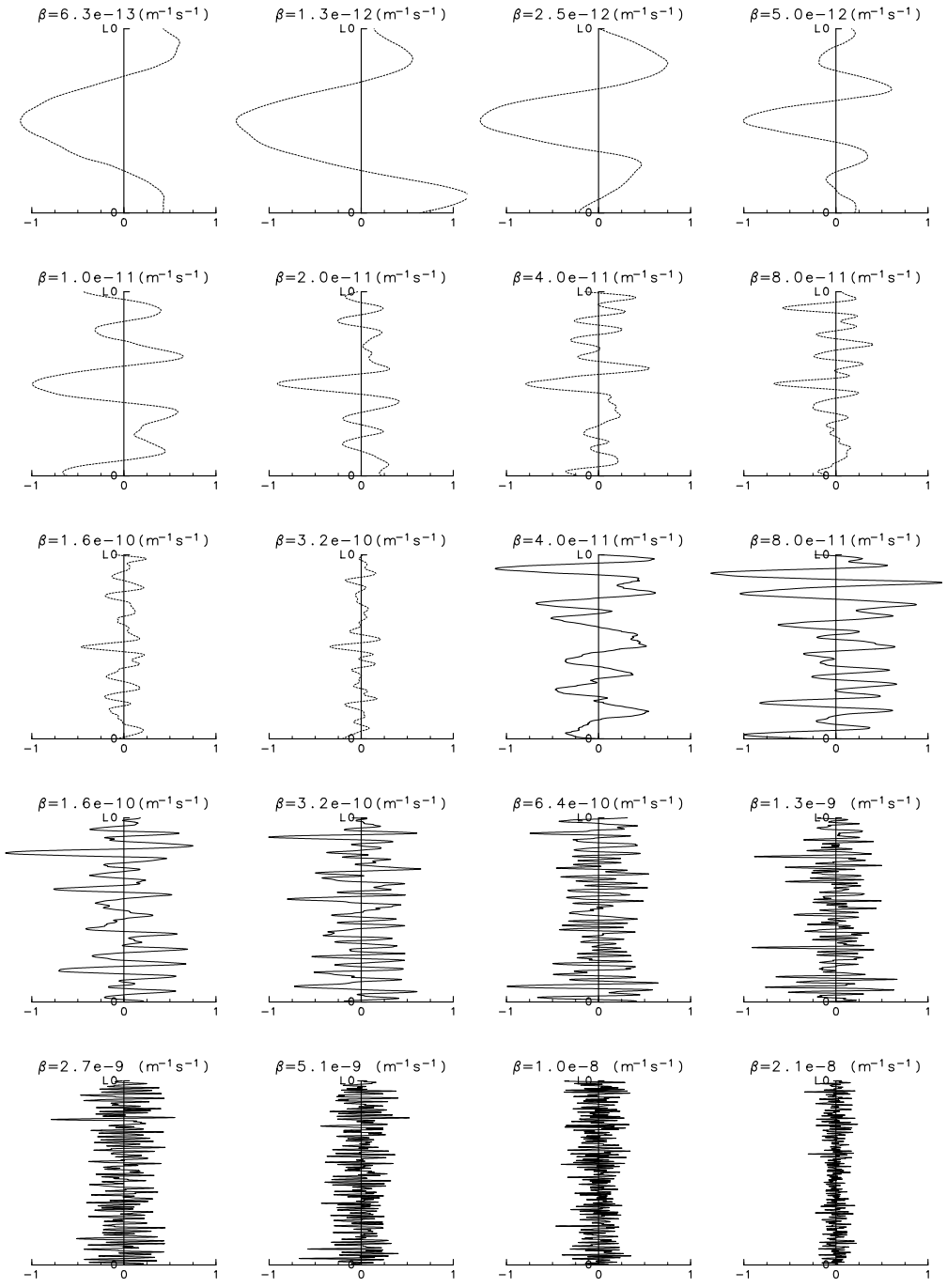

Figure 4: Meridional profiles the zonal mean zonal flow $[u](y,t)$ at $t = 12$ for different value of β. First 10 plots are enlargement of 1/8 part of the second 10 plots including the maximum $|[u]|$.

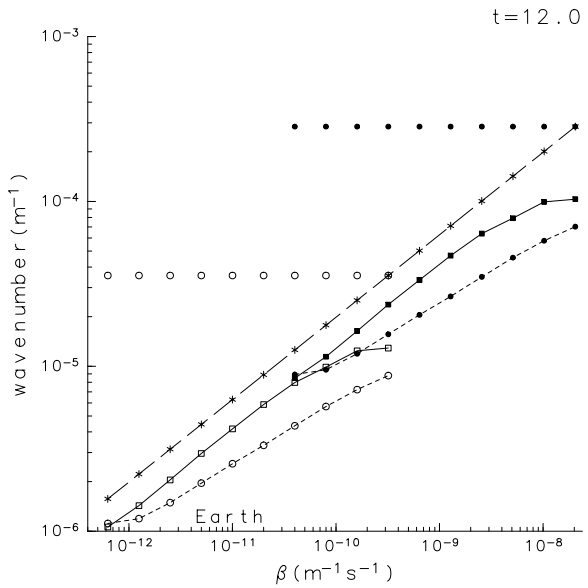

Figure 5: Energy centroid wavenumber (short broken line) and that only for $k = 0$ component (solid line) at $t = 12$ for different value of β^* with dimension. Long broken line gives k^*_β. Spectral peak at the initial state are also marked by closed or open circles.

Figure 5 summarizes the dependence of the meridional scale on β^*. Energy centroid wavenumber for $k = 0$ component is nearly parallel to k_β in a wide range of β^*; the meridional wavenumber increases in proportion to $\sqrt{\beta^*}$. In the cases in which k_β is not very different from κ_0, the proportionality breaks and the meridional wavenumber becomes much smaller than k_β.

4 Wave-mean flow interaction

Development of the zonal mean jet is diagnosed with a weakly nonlinear theory of interactions between Rossby waves and mean flow [24]. We expand each dependent variable with a small parameter ϵ:

$$\begin{aligned} u &= U + \epsilon u' + \epsilon^2 u^{(2)} + \cdots, \\ v &= \epsilon v' + \epsilon^2 v^{(2)} + \cdots, \\ \psi &= \Psi + \epsilon \psi' + \epsilon^2 \psi^{(2)} + \cdots, \\ \zeta &= Z + \epsilon \zeta' + \epsilon^2 \zeta^{(2)} + \cdots. \end{aligned}$$

Substituting these into Eq.(1) and neglecting the viscosity term, we obtain the following $O(\epsilon)$ vorticity equation:

$$\frac{\partial \zeta'}{\partial t} + U \frac{\partial \zeta'}{\partial x} + \hat{\beta} v' = 0, \tag{5}$$

where $\hat{\beta} = \beta - \partial^2 U / \partial y^2$. $O(\epsilon)$ enstrophy equation is obtained by multiplying ζ' to Eq.(5):

$$\frac{\partial}{\partial t} \frac{\zeta'^2}{2} + U \frac{\partial}{\partial x} \frac{\zeta'^2}{2} + \hat{\beta} v' \zeta' = 0, \tag{6}$$

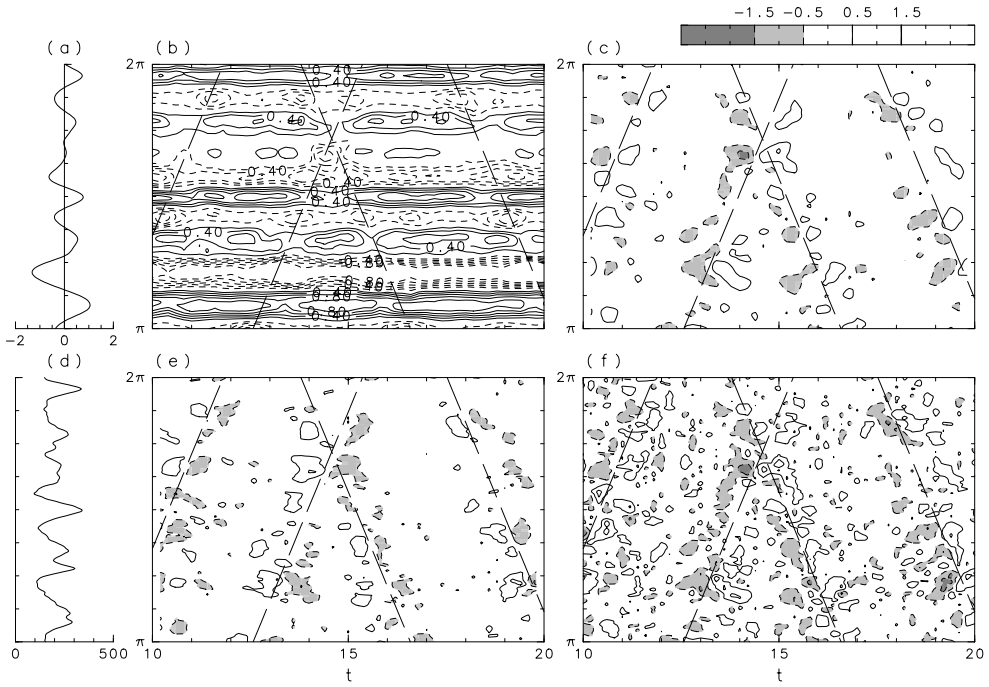

Figure 6: Diagnosis of wave-mean flow interactions for a run with a low-resolution model ($\beta = 200$). (a) time mean of the zonal mean zonal flow $\overline{[u]}(y)$ for $10 \leq t \leq 20$, (b) time evolution of the zonal mean zonal flow $[u](y,t)$, (c) time evolution of $\partial[u]/\partial t$, (d) time mean of $\hat{\beta} = \beta - d^2\overline{[u]}/dy^2$, (e) time evolution of the time-change of zonal mean wave activity $\partial[A]/\partial t$, and (f) time evolution of the divergence of wave activity flux $[\nabla \cdot \boldsymbol{F}] = [v'\zeta']$.

After some manipulation a wave activity equation is obtained as follows:

$$\frac{\partial A}{\partial t} + \nabla \cdot \boldsymbol{F} = 0, \tag{7}$$

where the wave activity is given by $A = \zeta'^2/(2\hat{\beta})$ and its flux by $\boldsymbol{F} = (UA + (v'^2 - u'^2)/2, -u'v')$. On the other hand, zonal mean of the zonal momentum equation for $O(\epsilon^2)$ becomes

$$\frac{\partial}{\partial t}[u^{(2)}] - [v'\zeta'] = 0. \tag{8}$$

Eliminating $[v'\zeta'] = [\nabla \cdot \boldsymbol{F}]$ in Eqs.(7) and (8), we obtain the conservation law of pseudo-momentum:

$$\frac{\partial}{\partial t}\Big\{[u^{(2)}] + [A]\Big\} = 0. \tag{9}$$

Firstly, interactions between Rossby waves and the zonal mean zonal flow are diagnosed after the development of the mean zonal flow in a low-resolution model of $k_m = l_m = 128$ with $\beta = 200$. Figure 6(a) shows the time mean of the zonal mean zonal flow $\overline{[u]}(y)$ for $10 \leq t \leq 20$, and (b) shows its time evolution $[u](y,t)$. The zonal mean jets are well developed by $t = 10$ and persists robustly over the following period. Deceleration and acceleration of the zonal mean jets propagate rather constantly in either latitudinal direction as shown in (c). The

time-change of the zonal mean wave activity $\partial[A]/\partial t$ (e) almost compensates $\partial[u]/\partial t$, and is associated with the divergence of wave activity flux $\nabla \cdot \boldsymbol{F}$ (f). These plots indicate the usefulness of the wave-mean flow interaction theory in diagnosing the time variation of the zonal mean jets after their development.

5 Concluding remarks

The formation of zonal jets in two-dimensional decaying turbulence on a β-plane is investigated in a wide parameter range of β. Their latitudinal scale becomes small as $\propto 1/\sqrt{\beta}$. Extremely persistent nature of the jets is reconfirmed in the present study with a high-resolution model. A weakly nonlinear Rossby wave-zonal flow interaction theory is a useful tool to diagnose the time variation of the zonal mean jets after their development. It is our next step to apply this tool to predict the latitudinal position and timing of the zonal jet formation.

References

[1] J. C. McWilliams, The emergence of isolated coherent vortices in turbulent flow, J. Fluid Mech., **146** (1984) 21–43.

[2] J. C. McWilliams, The vortices of 2-dimensional turbulence, J. Fluid Mech., **219** (1990) 361–385.

[3] P. B. Rhines, Waves and turbulence on a beta-plane, J. Fluid Mech., **69** (1975) 417–443.

[4] J. Pedlosky, *Geophysical Fluid Dynamics*, 2nd edn. (Springer, New York 1987) 710pp.

[5] M. E. Maltrud and G. K. Vallis, Energy-spectra and coherent structures in forced 2-dimensional and beta-plane turbulence, J. Fluid Mech., **228** (1991) 321–342.

[6] G. K. Vallis and M. E. Multrad, Generation of mean flows and jets on a beta plane and over topography, J. Phys. Oceanogr., **23** (1993) 1346–1362.

[7] R. L. Panetta, Zonal jets in wide baroclinically unstable regions: Persistence and scale selection, J. Atmos. Sci., **50** (1993) 2073–2106.

[8] G. P. Williams, Planetary circulations, 1. Barotropic representation of Jovian and terrestrial turbulence, J. Atmos. Sci., **35** (1978) 1399–1426.

[9] S. Yoden and M. Yamada, A numerical experiment on two-dimensional decaying turbulence on a rotating sphere, J. Atmos. Sci., **50** (1993) 631–643.

[10] J. Y-K. Cho and L. M. Polvani, The emergence of jets and vortices in freely evolving, shallow-water turbulence on a sphere, Phys. Fluids, **8** (1996) 1531–1552.

[11] T. Nozawa and S. Yoden, Formation of zonal band structure in forced two-dimensional turbulence on a rotating sphere, Phys. Fluids, **9** (1997) 2081–2093.

[12] T. Nozawa and S. Yoden, Spectral anisotropy in forced two-dimensional turbulence on a rotating sphere, Phys. Fluids, **9** (1997) 3834–3842.

[13] H.-P. Huang and W. A. Robinson, Two-dimensional turbulence and persistent zonal jets in a global barotropic model, J. Atmos. Sci., **55** (1998) 611–632.

[14] S. Yoden, K. Ishioka, Y.-Y. Hayashi and M. Yamada, A further experiment on two-dimensional decaying turbulence on a rotating sphere, Il Nuovo Cimento, **22 C** (1999) 803–812.

[15] K. Ishioka, M. Yamada, Y.-Y. Hayashi and S. Yoden, Technical approach for the design of a high-resolution spectral model on a sphere: Application to decaying turbulence, Nonlinear Processes in Geophys., **7** (2000) 105–110.

[16] J. Y-K. Cho and L. M. Polvani, The morphogenesis of bands and zonal winds in the atmospheres on the giant outer planets, Science, **273** (1996) 335–337.

[17] T. E. Dowling and E. A. Spiegel, Stellar and Jovian vortices, *NonLinear Astrophysical Fluid Dynamics*, Ann. New York Acad. Sci., (1990) 190–216.

[18] M. S. Miesch, Numerical modeling of the solar tachocline. I. Freely evolving stratified turbulence in a thin rotating spherical shell, Astrophys. J., **562** (2001) 1058–1075.

[19] D. W. J. Thompson and J. M. Wallace, The Arctic Oscillation signature in the wintertime geopotential and temperature fields, Geophys. Res. Lett., **25** (1998) 1297–1300.

[20] D. W. J. Thompson and J. M. Wallace, Annular modes in the extratropical circulation. Part I: month-to-month variability, J. Climate, **13** (2000) 1000–1016.

[21] D. L. Hartmann, J. M. Wallace, V. Limpasuvan, D. W. J. Thompson and J. R. Holton, Can ozone depletion and global warming interact to produce rapid climate change? Proc. Nat. Acad. Sci. **97** (2000) 1412–1417.

[22] P. B. Rhines, 'Rossby Waves and the Polar Vortex',

In, *http://www.ocean.washington.edu/research/gfd/rossby.html* (1998)

[23] P. B. Rhines, Jets, Chaos, **4** (1994) 313–229.

[24] Y-Y. Hayashi, K. Ishioka, M. Yamada and S. Yoden, 'Emergence of circumpolar vortex in two dimensional turbulence on a rotating sphere', In, *IUTAM Symposium on Developments in Geophysical Turbulence*. ed. by R.M. Kerr and Y. Kimura (Kluwer Academic Pub., Dordrecht, 2000) pp. 179–192.

[25] W. M. Washington and C. L. Parkinson, *An introduction to three-dimensional climate modeling*, (University Science Books, Mill Valley 1986) 422pp.